Low-temperature dielectric susceptibility of Li, Na, K, and Ag β-alumina

P. J. Anthony* and A. C. Anderson
Department of Physics and Materials Research Laboratory, University of Illinois at Urbana-Champaign, Urbana, Illinois 61801
(Received 17 October 1978)

Crystalline Na, K, Li, and Ag β-alumina show glasslike variations of the dielectric susceptibility with temperature and frequency provided the measuring field is directed along the conducting planes. Only Li β-alumina shows variations of the dielectric susceptibility perpendicular to the conducting planes. The data are discussed in terms of the tunneling-states model of amorphous materials. The estimated average tunneling distances are $\lesssim 0.3$ Å.

I. INTRODUCTION

In amorphous materials, a broad spectrum of low-energy ($\lesssim 10$ K) thermal excitations results in a specific heat[1,2] varying roughly linearly with temperature below ≈ 1 K, a phonon thermal conductivity[1,3] varying as $\approx T^2$, and unusual temperature, frequency, and nonlinear effects in the ultrasonic[4,5] and dielectric[6-8] properties at low temperatures. The excitations are most successfully explained by a tunneling-states model[9,10] in which the excitations arise from quantum-mechanical tunneling of some entities of the glass which reside in double-well potentials. A variety of experiments on vitreous silica are adequately explained quantitatively[11-13] by this model.

In single crystals of Li, Na, K, and Ag β-alumina a linear specific heat[14,15] has also been observed, and a T^2 thermal conductivity[16] is found in single crystals of Li, Na, and Ag β-alumina. The present work[17] sought further evidence in β-alumina of the characteristically glasslike excitations through measurements of the low-temperature dielectric constant ϵ. The results, along with a recent observation of saturation effects[18] in the dielectric behavior of Na β-alumina, confirm the glasslike character of the β-aluminas. However, we find that the low-temperature properties of β-alumina are not accounted for quantitatively using the tunneling-states model with assumptions found to be adequate for explaining the properties of vitreous silica.[12]

M β-alumina[19,20] is a two-dimensional superionic conductor. It has a layered, crystalline structure composed of ≈ 8-Å-thick slabs of alumina separated by ionically conducting planes. These planes contain both spacer oxygen atoms, which are covalently bonded between the slabs, and the mobil, monovalent cations M, where M = Li, Na, K, Ag, etc. The crystal composition is nonstoichiometric, i.e., there is roughly a (15–30)% excess of cations in the conducting planes plus a corresponding number of oxygens to balance charge. Thus the conducting planes are highly disordered. Specific-heat[14,15] and thermal-conductivity[16] measurements indicated that the low-energy localized excitations are confined to the conducting planes, and hence the "glassy" regions should be two dimensional. Indeed, the lower dimensionality is apparent in the anisotropy of the dielectric properties reported in this paper.

Section II describes the preparation of samples and the experimental techniques, and presents the data. Section III reviews the appropriate portions of the tunneling-states model and compares this model with the data.

II. EXPERIMENTAL

A 2.5-cm length cut from a 2.5-cm-diam boule of single-crystal Na β-alumina was acquired from Union Carbide.[21] The crystal was grown from the melt by the Czochralski method,[22] had several small, visible inclusions in one section, and had a number of surface cracks.[22] As a test of crystal quality, the ionic conductivity was measured using salt-water contacts at a frequency of 10^4 Hz at 300 K. The result was $\approx 10^{-2}\ \Omega^{-1}\ \mathrm{cm}^{-1}$ which is in rough agreement with other measurements on melt grown crystals.[19] Samples were cut from the boule using a diamond saw under kerosene. In some samples, the Na ions were replaced[23] by Li, K, or Ag by immersion in the appropriate nitrate salt at $\approx 350\,^\circ$C. The fused salt left on the surface was removed with a brief water rinse and precipitated metallic silver was removed with dilute nitric acid. Density changes obtained with ion exchange, together with neutron activation analyses, indicated an $\approx 17\%$ excess of cations over stoichiometry, or ≈ 2.3 cations per unit cell. Several of the capacitance measurements were made on samples used previously for thermal conductivity or specific-heat measurements.[24]

For capacitance measurements with the measuring field directed paralled to the crystalline c axis ($\vec{E} \parallel \vec{c}$), i.e., perpendicular to the conducting

planes, ≈0.5-mm sections were cut or cleaved from larger crystals. For measurements with the field directed perpendicular to the c axis ($\vec{E} \perp \vec{c}$), large Na or Ag crystals were first potted in epoxy,[25] then ≈0.5 mm sections were sliced off using a diamond wire saw and mineral-oil lubricant. The epoxy coating prevented massive fracturing of the sample. To provide sufficient area for the capacitor, several smaller pieces of Li or K β-alumina were glued together with epoxy[25] and then sectioned.

Vapor-deposited In was used for the electrodes; the resulting capacitance was ≈10 pF. The epoxy used to bind the $\vec{E} \perp \vec{c}$ samples contributed less than 5% of the capacitance and, when measured separately, had a factor of 10^2 smaller variation in dielectric constant with variations of temperature and frequency than the β-alumina.

Capacitance measurements were made within a copper box used for electrical shielding; see Fig. 1. The inner surface of one wall of the box was electrically insulated with a covering of cigaret paper and Ge7031 varnish. The samples were thermally grounded to this surface using Apiezon N grease. Manganin leads were attached to the In electrodes with silver paint. The lead to the thermally grounded electrode served as the unshielded, high-potential connection in a three-terminal capacitance measurement.[26] The low-potential lead entered the box through an electrically grounded coaxial shield—these provided the other two connections for the three-terminal

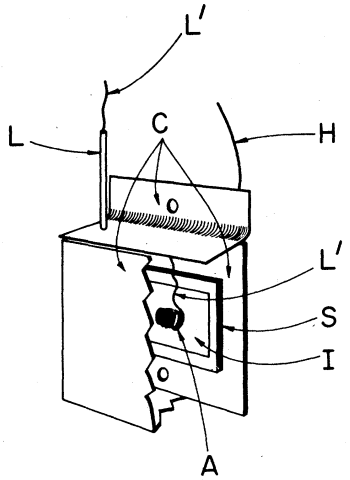

FIG. 1. Sample mounting arrangement for capacitance measurements. C, copper shielding box; S, capacitor sample with indium electrodes I on both sides; L, outer shield of coaxial line, connected to C; L', inner lead of coax connected to indium electrode with silver paint, A; H, lead connected to reverse side of capacitor with silver paint.

measurement. The leads were thermally grounded before entering the copper box.

Measurements on a sapphire-crystal capacitor of similar construction showed less than $2/10^4$ change in capacitance for variation in voltage of 0.06–6 V, in frequency of 10^2–10^4 Hz, or in temperature of 0.02–10 K. Near 0.02 K a 6 V measuring potential did heat some β-alumina samples by <5%. Hence measurements were made at 0.6 V which provided a precision of $3/10^5$. Guard rings were not employed for the measurements since absolute measurements of capacitance were not required. However, the In electrodes were generally set back from the sample edges a distance equal to the sample thickness to keep fringing fields in the measured medium. This did effect the orientation of the measurements slightly, introducing an estimated 1% of $\vec{E} \perp \vec{c}$ character to the $\vec{E} \parallel \vec{c}$ measurements and ≲5% of $\vec{E} \parallel \vec{c}$ character to $\vec{E} \perp \vec{c}$ measurements because of the sample geometries involved.

Temperatures below ≈2 K were provided by germanium resistance thermometers[27] calibrated from a cerium magnesium nitrate magnetic thermometer.[28] The magnetic thermometer was calibrated[29] against a U. S. Natl. Bur. Stand. superconducting fixed-point device.[30] Temperatures above ≈2 K were provided by commercially calibrated germanium resistance thermometers.

At temperatures above ≈30 K, capacitance measurements are complicated by a large ionic conductivity.[23] Below ≈30 K, however, the cations are well localized as deduced from their activation energies.[19] This is evident from the conductivity data for Na β-alumina shown in Fig. 2. Hence our measurements are confined to temperatures less than ≈30 K.[36–38]

The dielectric-constant data at low temperatures for M β-alumina with $\vec{E} \perp \vec{c}$ are plotted in Figs. 3–6 as a function of temperature for several frequencies. Microwave data by Strom *et al.*[18] are included for Na β-alumina in Fig. 3. Variations with frequency and temperature for Na, Ag, and K β-alumina with $\vec{E} \parallel \vec{c}$ between 0.02 and 4 K and for 10^2–10^4 Hz were less than 7, 30, and 0.7 parts in 10^4, respectively, and thus have not been plotted. The slight variations with temperature for $\vec{E} \parallel \vec{c}$ arise from $\vec{E} \perp \vec{c}$ through the fringing fields as discussed above. Hence, to the precision of our measurements, there is *no* temperature variation of ϵ in Na, Ag, or K β-alumina for a uniform measuring field directed parallel to the c axis. The data for Li β-alumina with $\vec{E} \parallel \vec{c}$ do, however, show large variations with frequency and temperature as indicated in Fig. 7. For any cation, changes in measuring voltage of 0.06–6 V produced less than $2/10^3$ variation in ϵ at any temperature or frequency.

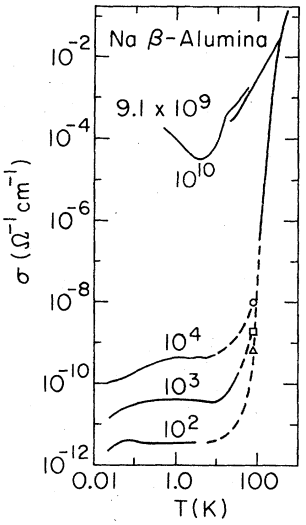

FIG. 2. Conductivity vs temperature at several frequencies for Na β-alumina with $\vec{E} \perp \vec{c}$. Data at 10^2–10^4 Hz taken in conjunction with the dielectric-constant measurements. O, 10^4; □, 10^3; △, 10^2 Hz at 77 K from Ref. 36. Data at 9.1×10^9 Hz from Ref. 37, 1.2×10^{10} Hz from Ref. 18, and high-temperature data (10^4–10^{11} Hz) from Ref. 38.

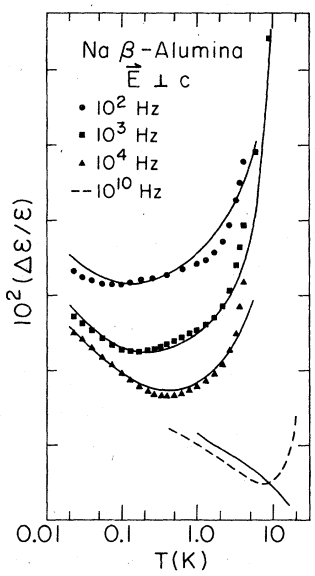

FIG. 3. Variation of dielectric constant in units of $10^2\,\Delta\epsilon/\epsilon$, vs temperature of Na β-alumina, measured relative to a fixed but arbitrary value of ϵ with $\vec{E} \perp \vec{c}$, from 10^2 to 10^4 Hz for a measuring field of 3.3 V/cm rms. The dashed line is from the data of Ref. 18, and has been adjusted on the vertical, linear scale. The data for 10^2–10^4 Hz have not been so adjusted and thus reflect the measured frequency dependences. The solid lines are calculated using the parameters of Table I as described in the text. The curves for 10^2 and 10^3 Hz have been offset from the 10^4-Hz curve by 10^{-2} and 3×10^{-3}, respectively.

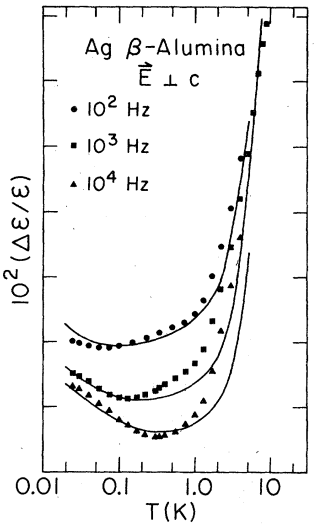

FIG. 4. Variation of dielectric constant in units of $10^2\,\Delta\epsilon/\epsilon$, vs temperature of Ag β-alumina with $\vec{E} \perp \vec{c}$, from 10^2 to 10^4 Hz for a field of 4.5 V/cm. The solid lines are calculated using the parameters of Table I as described in the text. The curves for 10^2 and 10^3 Hz have been offset from the 10^4-Hz curve by 9×10^{-3} and 3×10^{-3}, respectively.

III. DISCUSSION

The variations in the low-temperature dielectric constant of β-alumina have nearly the same frequency and temperature characteristics as the

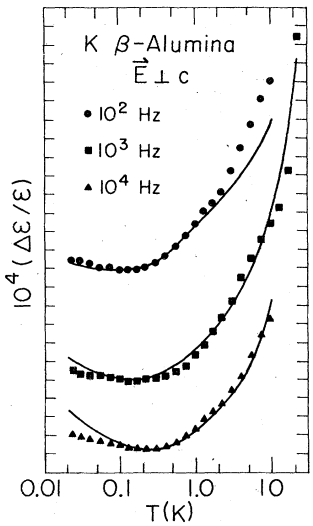

FIG. 5. Variation of dielectric constant, in units of $10^4\Delta\epsilon/\epsilon$, vs temperature of K β-alumina with $\vec{E} \perp \vec{c}$, from 10^2 to 10^4 Hz at a field of 4.6 V/cm. The solid lines are calculated using the parameters of Table I as described in the text. The curves for 10^2 and 10^3 Hz have been offset from the 10^4-Hz curves by 8.0×10^{-4} and 3.0×10^{-4}, respectively.

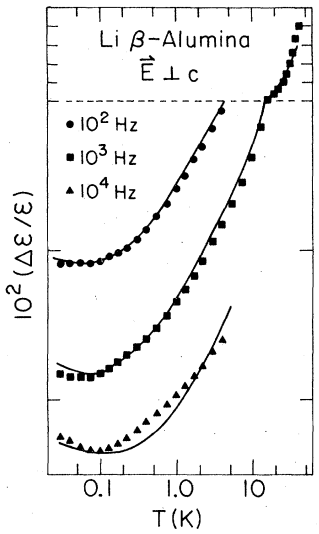

FIG. 6. Variation of dielectric constant, in units of $10^2\Delta\epsilon/\epsilon$, vs temperature of Li β-alumina with $\vec{E}\perp\vec{c}$, from 10^2 to 10^4 Hz for a field of 7.0 V/cm. Note the factor-of-8 change in vertical scale for the high-temperature data. The solid lines are calculated using the parameters of Table I as described in the text. The curves for 10^2 and 10^3 Hz have been offset from the 10^4-Hz curve by 9.3×10^{-3} and 3.8×10^{-3}, respectively.

variations found in glasses.[7,13] The variations are similar in magnitude to those observed[13] in the borosilicate glass BK7. There is, however, one major difference between the variations in β-alumina versus those in glasses, namely, the anisotropy. For Na, K, and Ag β-alumina the variations for the electric field oriented $\vec{E}\perp\vec{c}$ are large and similar to bulk glasses, while the susceptibility with $\vec{E}\parallel\vec{c}$ is nearly constant as for a pure crystal.

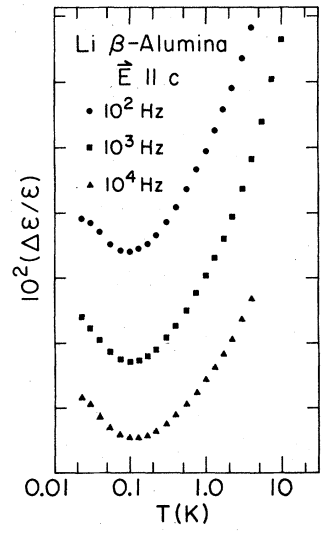

FIG. 7. Variation of dielectric constant, in units of $10^2\,\Delta\epsilon/\epsilon$, vs temperature of Li β-alumina with $\vec{E}\parallel\vec{c}$, from 10^2 to 10^4 Hz for a field of 2.8 V/cm. Unlike Na, Ag, and K β-alumina, large variations are observed Li β-alumina with the measuring field applied perpendicular to the conducting planes.

Thus, the β-aluminas contain a broad spectrum of low-energy, localized excitations similar in behavior to the excitations found in amorphous materials. This conclusion is based on specific heat,[14,15] thermal transport,[16] electric saturation,[18] and the present dielectric-dispersion measurements. Furthermore, from the effects of ion exchange it is clear that the excitations in β-alumina involve only ions associated with the conducting planes. Finally, the charge motion associated with the excitations in β-alumina, except for Li β-alumina, is itself confined or parallel to the conducting planes.

For Li β-alumina the dielectric variation for $\vec{E}\parallel\vec{c}$, rather than being negligible as for the other β-aluminas, is actually larger than for $\vec{E}\perp\vec{c}$. This may result from the small size of the Li^+ ion which allows it to move off the mirror plane towards either alumina slab by a distance[31] of 0.85 Å. Thus, the Li ion may move back and forth across the conducting plane, parallel to the c axis.

A quantitative explanation of the data can be sought in the phenomenological tunneling-states model developed for glasses. The model will be applied not only to the present dielectric-dispersion data, but also to the earlier specific-heat and thermal-transport data since all measurements involved the same set of samples.

The tunneling-states model as originally proposed by Anderson, Halperin, and Varma[9] and by Phillips[10] was intended to explain the linear specific heat, the low thermal conductivity, and the discrepancy in directly measured and deduced phonon mean free paths in glasses. The model envisions that the localized excitations responsible for the anomalous glassy properties are some units of the glass that reside in double-well potentials. The weak overlap of the ground-state wave functions in the two individual minima, plus the asymmetry ξ between these minima, give rise to a small energy splitting E between the ground state and the first excited state of the combined system. The splitting is given by $E=(\Delta^2+\xi^2)^{1/2}$, where the overlap energy Δ varies with the well separation $2d$, the height V of the potential-energy barrier, and the mass m of the tunneling unit.

In principle, one could obtain a density of tunneling states[32] $P(\xi,\lambda)$ in terms of the double-well parameters ξ and λ. [The parameter $\lambda=(2mV)^{1/2}d/\hbar$ and $\Delta\approx(2V/\lambda)e^{-\lambda}$.] Experimentally, however, the density $P(E,\tau)$ is more accessible, where τ is the relaxation time of a tunneling state of energy

E. It has been suggested[4] that τ arises primarily through a modulation $\delta\xi$ in the asymmetry ξ by the strain e of a passing acoustic phonon. Assuming the coupling parameter $\gamma = \frac{1}{2}(\delta\xi/\delta e)$ is essentially independent[4] of E, then[32]

$$\tau^{-1} = \sum_i \left(\frac{2\gamma_i^2}{\rho v_i^2}\right) (4\pi\hbar^4 v_i^3)^{-1} \Delta^2 E \coth\left(\frac{E}{2kT}\right), \quad (1)$$

where ρ is the mass density, v is the acoustic phonon velocity, and the summation is over the three acoustic-phonon modes. Equation (1) provides a spectrum of τ values for each tunneling energy E.

Generally, it is assumed for convenience that $P(\xi,\lambda)$ is a constant independent of ξ and λ. Here, however, we shall allow $P(\xi,\lambda) = P(E)$, which has at most only a weak dependence on τ. Then[32]

$$P(E,\tau) = (2\tau)^{-1}(1-\tau_{\min}/\tau)^{-1/2} P(E), \quad (2)$$

where $\tau_{\min} = (\Delta/E)^2\tau$ is the shortest relaxation time that occurs in the sample for states of energy E, which occurs when $\Delta = E$. The specific heat in excess of the phonon (Debye) specific heat is then

$$C_{ex} = \int_0^{E_{\max}} dE\, E^2 \left[4kT^2 \cosh^2\left(\frac{E}{2kT}\right)\right]^{-1} P(E)\eta(E), \quad (3)$$

where $\eta(E)$ represents[11] the quantity $\frac{1}{2}\ln(4\tau_{\max}/\tau_{\min})$. Note that the time scale of the experiment determines $\tau_{\max}$ if the distribution over τ extends to that time scale.

There are two processes in the tunneling-states model which contribute to the absorption of electromagnetic waves, analogous to the resonant and relaxation scattering mean free paths of phonons.[4] The resonant absorption[6] of electromagnetic waves with $\omega = E/\hbar$ is

$$\alpha_{res} = \pi^2(\epsilon+2)^2\mu_0^2(27\epsilon\hbar c)^{-1} E \tanh(E/2kT) P(E), \quad (4)$$

where μ_0 is the average microscopic dipole moment of the two-level states and c is the velocity of light. Use has been made here of the Lorentz local-field approximation to relate the macroscopic dipole moment to μ_0, and it has been assumed that the primary modulation of the state by the field is through the asymmetry energy ξ. The absorption of electromagnetic waves[7] analogous to the relaxation scattering of phonons is

$$\alpha_{rel} = \frac{\pi\mu_0^2(\epsilon+2)^2}{54\epsilon kTc} \int_0^{E_{\max}} \frac{dE\, P(E)}{\cosh^2(E/2kT)} \times \int_{\tau_{\min}}^{\tau_{\max}} \frac{d\tau\,(1-\tau_{\min}/\tau)^{1/2}\omega_0^2}{1+\omega_0^2\tau^2}. \quad (5)$$

Equation (5) displays explicitly the dependence of the relaxation process on a spectrum of τ values.

If we now let

$$B_\epsilon = (-2\pi/27)\mu_0^2(\epsilon_0+2)^2/\epsilon_0$$

and

$$A = 2\pi\hbar^4\rho v^2\gamma^{-2}(k^3\textstyle\sum_i v_i^{-3})^{-1}\omega_0,$$

the electromagnetic dispersion can be related[6] to the absorption by the Kramers-Kronig relation, with $\Delta\epsilon/\epsilon = (\Delta\epsilon/\epsilon)_{res} + (\Delta\epsilon/\epsilon)_{rel}$,

$$\left(\frac{\Delta\epsilon}{\epsilon}\right)_{res} = \left(B_\epsilon \int_0^{E_{\max}/kT} \frac{dx\, x\tanh(\frac{1}{2}x)P(xkT)}{(h\omega_0/kT)^2 - x^2}\right) - \left(B_\epsilon \int_0^{E_{\max}/kT'} \frac{dx\, x\tanh(\frac{1}{2}x)P(xkT')}{(h\omega_0'/kT')^2 - x^2}\right) \quad (6)$$

and

$$\left(\frac{\Delta\epsilon}{\epsilon}\right)_{rel} = \left(-\frac{B_\epsilon}{4}\int_0^{E_{\max}/kT} \frac{dx\,P(xkT)}{\cosh^2(\frac{1}{2}x)} \int_0^{\ln(\tau_{\max}/\tau_{\min})} \frac{ds\,(1-e^{-s})^{1/2}}{1+A^2\tanh^2(\frac{1}{2}x)e^{2s}(xT)^{-6}}\right)$$

$$-\left(\frac{B_\epsilon}{4}\int_0^{E_{\max}/kT'} \frac{dx\,P(xkT')}{\cosh^2(\frac{1}{2}x)} \int_0^{\ln(\tau_{\max}/\tau_{\min})} \frac{ds\,(1-e^{-s})^{1/2}}{1+(A\omega_0'/\omega_0)^2\tanh^2(\frac{1}{2}x)e^{2s}(xT')^{-6}}\right). \quad (7)$$

For $\hbar\omega_0 \ll kT$ and a constant density of states, Eq. (6) provides a logarithmic decrease of $\Delta\epsilon/\epsilon$, while Eq. (7) increases $\Delta\epsilon/\epsilon$ with increasing temperature.

For a density of states independent of E, the tunneling-states model gives $C \propto T$ and $\kappa \propto T^2$. These are nearly, but not exactly, the dependences observed experimentally, and an energy dependent $P(E)$ was suggested[2] to account for the differences. Therefore, we assume a form of $P(E,\tau)$ such that

$$\eta(E)P(E) = \begin{cases} P_m(E/kT_N)^m + P_n(E/kT_N)^n & \text{for } E < E_{\max} \\ 0 & \text{for } E > E_{\max}. \end{cases} \quad (8)$$

The energy E has been normalized by dividing by kT_N, where $T_N = 1$ K. The coefficients P_m and P_n are constants. As an example, m and n are roughly 0.3 and 3, respectively, for vitreous silica.[12] This certainly is not a unique representation of $P(E)$, but it does provide reasonable agreement with experimental measurements on vitreous sil-

TABLE I. Summary of parameters for M β-alumina. All parameters and their sources are described in the text.

Parameter	Units	Na	Ag	K	Li
ρ [a]	$g\,cm^{-3}$	3.22	3.74	3.33	3.14
v_t [a]	$10^5\ cm\ sec^{-1}$	3.8	3.6	4.3	4 [b]
v_l [a]	$10^5\ cm\ sec^{-1}$	9.1	8.8	9.5	9 [b]
t	sec	5	5	5	5
ϵ [c]	...	11.9	11.1	11 [b]	11 [b]
τ_{max}/τ_{min}	...	10^6	10^6	10^6	10^6
m	...	0.2	0.2	0.2	0.2
n	...	3.0	3.0	3.0	3.0
P_m	$10^{33}\ erg^{-1}\,cm^{-3}$	2.4	4.4	1.2	4.9
P_n	$10^{29}\ erg^{-1}\,cm^{-3}$	4.5	67	0.26	0.36
E_{max}/k	K	65	33	80	130
γ_l	eV	0.3	0.4	0.9	1.4
μ_0	D	1.3	1.0	0.4	1.1
γ_l'	eV	0.2	0.3	0.1	0.6

[a] From Ref. 34.
[b] Estimated from the values for other cations.
[c] From Ref. 33.

ica[12] while still being mathematically convenient.

A number of parameters in the model are essentially constants. The density ρ was measured for each β-alumina to 1%. The quantity $\eta(E)$ is not a separate parameter but is determined by the other parameters. The time scale t of the specific-heat experiment enters the quantity $\eta(E)$ only logarithmically and thus is adequately determined. The normalized coupling parameter $(2\gamma_l^2/\rho v_l^2)$ is assumed[4] to have the same value for the three phonon polarizations. For Na and Ag β-alumina the low-frequency dielectric constant ϵ has been determined.[33] The average acoustic-phonon velocities of Na, Ag, and K β-alumina are available[34] from the elastic constants. The values of the constant parameters ($\rho, v_t, t,$ and ϵ) are listed at the top of Table I.

Several parameters were kept fixed for all the β-aluminas. The frequency dependence of the relaxation process varies weakly with the exact magnitude of the ratio τ_{max}/τ_{min} when this ratio is large, and thus τ_{max}/τ_{min} was not varied. The energy dependences, m and n, of the density of states [Eq. (8)] were kept fixed for all cation species, m on the basis of the similar temperature dependences of the low-temperature specific heats. Because the physical properties being calculated primarily depend on the number of higher-energy states and not the exact temperature dependence of the density of states, the parameter n of the density $P_n(E/k)^n$ in Eq. (8) was not varied. The values of the three parameters kept fixed for all the β-aluminas (τ_{max}/τ_{min}, m and n) are listed in the middle of Table I.

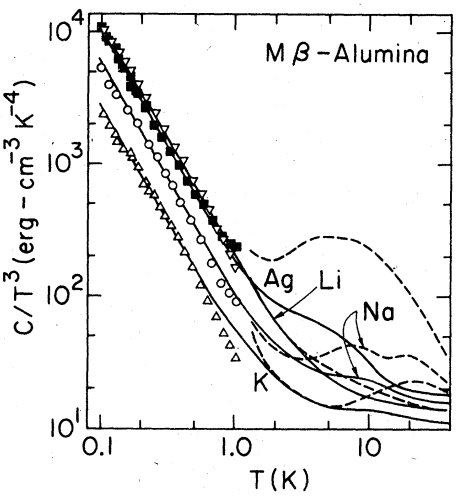

FIG. 8. Theoretical fits to the Debye plus excess specific heat, divided by T^3, vs temperature for M β-alumina. The solid lines are calculated using the parameters of Table I as described in the text. Data from Ref. 15 are denoted by ∇ for Li; ■, Ag; ○, Na; △, K. The dashed curves are from the data of McWhan *et al.*, Ref. 14. The specific heats at high temperatures are interpreted as being partially due to Einstein-oscillator contributions (see Ref. 14).

There remain five parameters which vary among the different β-aluminas. The magnitude P_m of the density of states at low energies [Eq. (8)] is set by the low-temperature specific heat. The temperatures of the minima in the variations of the dielectric constant determine the magnitude of the coupling parameter γ. The dipole moment μ_0 is set by the size of the variations with temperature of the dielectric constant at temperatures below $\approx$1 K. The higher temperature, more-rapid increase of the variation with temperature gives the approximate magnitude of the density of states at higher energies, P_n, and sets a lower limit on the arbitrary cutoff of the density, E_{max} [Eq. (8)].

The values of the five variable parameters (P_m, P_n, E_{max}, γ, and μ_0) used to fit the data are listed at the bottom of Table I. Note that for dipoles due to in-plane tunneling only, measured with $\vec{E} \perp \vec{c}$, a factor of $\frac{1}{3}$ in Eqs. (4) and (5) due to averaging $\cos^2\theta$ over three dimensions is to be replaced by a factor of $\frac{1}{2}$. Similarly, for tunneling only along the c axis and with $\vec{E} \parallel \vec{c}$, the $\frac{1}{3}$ is to be replaced by 1 in Eqs. (4) and (5).

The specific-heat data of Fig. 8 are, by the nature of the fitting procedure, well represented by the theory over the entire temperature range for Li β-alumina and up to roughly 1, 4, and 8 K for Ag, Na, and K β-alumina, respectively. The discrepancies above those temperatures are accounted for by McWhan *et al.*[14] using Einstein-oscilla-

tor contributions of known cation vibrations.

The theoretical fits to the $\vec{E} \perp \vec{c}$ measurements of the variations of dielectric constant are shown in Figs. 3–6. Although the tunneling-states model can provide an explanation for the temperature variations of the dielectric constant, a portion of the variations with frequency for all four cations is unexplained. That is, there is an additional frequency dependence of roughly the same size for Na, Li, and Ag β-alumina such that at temperatures below the minimum in $\Delta\epsilon/\epsilon$, the $\Delta\epsilon/\epsilon$ data do not approach a common asymptote as in glasses[7,13] and as required by the theory. Also, for the Li β-alumina, $\vec{E} \parallel \vec{c}$ data of Fig. 7, the present formulation of the model does not explain the minima, which do not vary with temperature for different measuring frequencies.

One other problem with the analysis occurs for the 10^{10}-Hz data for the variations of the susceptibility of Na β-alumina with $\vec{E} \perp \vec{c}$ (Fig. 3). If the minima scaled[7] as ω/T^3 from low frequencies, the minima for 10^{10}Hz would be expected to be at $\approx$40 K. However, that scaling law assumes a density of states that is relatively energy independent. A strong energy dependence would produce a minimum at lower temperatures. The low-frequency data do not require a sufficiently strong energy dependence to fit the 10^{10}-Hz data. Alternatively, an $E_{\max}/k$ of the order of 100 K would be needed to give a minimum near the observed temperature of 9 K.

The low-temperature[35] thermal conductivities of β-alumina[16] should now be explained by the model using the values listed in Table I with *no* additional adjustable parameters. However, satisfactory agreement with the thermal-conductivity data requires a different value for the coupling parameter γ, which is listed as γ' in Table I. Curves of $\Delta\epsilon/\epsilon$ calculated using γ' values would have minima which occur at temperatures too high by a factor of 2 for Na β-alumina and more than a factor of 10 for K β-alumina. The temperatures at which the minima occur are determined by the strong competition of the resonant and relaxation contributions. Thus, a small change in the magnitude of one process with respect to the other can radically alter the position and shape of the minima. The discrepancies could be due in part to assuming the same density of states for phonon and electromagnetic interactions, to assuming a single average value for both γ and μ_0 for all the tunneling states, or to assuming that $2\gamma^2/\rho v^2$ is the same for all phonon polarizations. Also, phonons traveling in different directions may not scatter equally well from the tunneling states confined to the two-dimensional planes, or phonon focusing may be influencing the thermal transport. Alternatively, acceptable fits to the dielectric data using the values of γ' deduced from the thermal conductivity data can be produced using a nonuniform distribution of tunneling-state parameters. This effectively introduces two separate dipole moments: the same μ_0 for the resonant process plus μ_0' for the relaxation process. For example, a fit similar to that shown in Fig. 5 for K β-alumina is found using $\mu_0' = 1.7\mu_0$ and $P_n = 0.18 \times 10^{29}$ erg^{-1} cm^{-3}.

In brief, the phenomenological tunneling-states model could be adjusted to fit the present data if constraints on the parameters on the model were further relaxed relative to the case of vitreous silica, as an example.

If the tunneling unit, active in the $\vec{E} \perp \vec{c}$ measurements, is assumed to possess a charge equivalent to one electron, the approximate average well separation would be 0.3, 0.2, 0.1, and 0.2 Å for Na, Ag, K, and Li β-alumina, respectively. Thus, the tunneling is probably not that of a cation tunneling from site to site,[14] a distance of $\approx$3 Å. The density of states deduced for the β-aluminas are comparable to those found for vitreous silica.[12] A *lower* bound on the *total* number of tunneling states per unit cell apparent in the three sets of measurements and fits is very roughly 0.2, 0.1, 0.04, and 0.3 for Na, Ag, K, and Li β-alumina, respectively, compared to 2.3 cations per unit cell. These values are very sensitive to the upper limit on the density of states $E_{\max}$ which enters as the fourth power. Nevertheless, it would appear that the major tunneling unit for all the β-aluminas is not the charge-compensating defect oxygens, which only number $\approx$0.15 per unit cell. The calculated number of tunneling units and the derived tunneling distances are not reliable enough, however, to discriminate between in-site cation tunneling, spacer oxygen tunneling, or a more complicated, cooperative tunneling of groups of ions. For Li β-alumina with $\vec{E} \parallel \vec{c}$ there is the possibility that the Li cation is tunneling across the mirror plane though a distance[31] of 1.7 Å. Only 2% of the excess excitations observed in the low-temperature specific heat of Li β-alumina would need to be due to tunneling along the c axis to produce the magnitude of the temperature variation of the $\vec{E} \parallel \vec{c}$ data shown in Fig. 7.

In summary, crystalline β-alumina contains a broad spectrum of localized excitations similar in behavior to excitations found in glassy materials. The excitations in β-alumina are confined to the conducting planes. The motion related to the excitations, at least in Na, K, and Ag β-alumina, is itself constrained to the conducting planes. The tunneling-states model which adequately accounts for the properties of fused silica, for example, does not quantitatively fit the β-alumina data if the

same assumptions are retained which were used to fit fused silica. Relaxation of these restrictions would provide agreement between the phenomonological theory and experiment, but then the parameters of the model are no longer overdetermined by existing experimental data.

ACKNOWLEDGMENT

This work was supported in part by the U. S. Department of Energy under Contract No. EY-76-C-02-1198.

---

*Present address: Bell Laboratories, Murray Hill, N.J. 07974.

[1]R. C. Zeller and R. O. Pohl, Phys. Rev. B 4, 2029 (1971).

[2]J. C. Lasjaunias, A. Ravex, M. Vandorpe, and S. Hunklinger, Solid State Commun. 17, 1045 (1975), and references cited.

[3]M. P. Zaitlin and A. C. Anderson, Phys. Rev. B 12, 4475 (1975).

[4]S. Hunklinger and W. Arnold, in *Physical Acoustics*, edited by W. P. Mason and R. N. Thurston (Academic, New York, 1976), Vol. 12, p. 155, and papers cited.

[5]For a recent review of ultrasonic properties of glasses, see, B. Golding, in *1976 Ultrasonic Symposium Proceedings* (IEEE, New York, 1976), p. 692.

[6]M. von Schickfus, S. Hunklinger, and L. Piche, Phys. Rev. Lett. 35, 876 (1975); M. von Schickfus and S. Hunklinger, J. Phys. C 9, L439 (1976).

[7]G. Frossati, J. le G. Gilchrist, J. C. Lasjaunias, and W. Meyer, J. Phys. C 10, L515 (1977).

[8]M. von Schickfus and S. Hunklinger, Phys. Lett. A 64, 144 (1977).

[9]P. W. Anderson, B. I. Halperin, and C. M. Varma, Philos. Mag. 25, 1 (1972).

[10]W. A. Phillips, J. Low Temp. Phys. 7, 351 (1972).

[11]J. L. Black and B. I. Halperin, Phys. Rev. B 16, 2879 (1977).

[12]T. L. Smith, P. J. Anthony, and A. C. Anderson, Phys. Rev. B 17, 4997 (1978).

[13]P. J. Anthony and A. C. Anderson (unpublished).

[14]D. B. McWhan, C. M. Varma, F.L.S. Hsu, and J. P. Remeika, Phys. Rev. B 15, 553 (1977).

[15]P. J. Anthony and A. C. Anderson, Phys. Rev. B 16, 3827 (1977).

[16]P. J. Anthony and A. C. Anderson, Phys. Rev. B 14, 5198 (1976).

[17]A preliminary account of a portion of this work was presented in Bull. Am. Phys. Soc. 23, 325 (1978).

[18]U. Strom, M. von Schickfus, and S. Hunklinger, Phys. Rev. Lett. 41, 910 (1978).

[19]For a recent review of β-alumina see, J. H. Kennedy, in *Topics in Applied Physics: Solid Electrolytes*, edited by S. Geller (Springer-Verlag, New York, 1977), Vol. 21, p. 105.

[20]*Superionic Conductors*, edited by G. D. Mahan and W. L. Roth (Plenum, New York, 1976), Sec. D.

[21]Union Carbide Corp., Crystal Products Division, 8888 Balboa Avenue, San Diego, Calif. 92123.

[22]L. R. Rothrock, J. Cryst. Growth 39, 180 (1977).

[23]J. T. Kummer, in *Progress in Solid State Chemistry*, edited by H. Reiss and J. O. McCaldin (Pergamon, New York, 1972), Vol. 7, p. 141, and references cited.

[24]P. J. Anthony, Ph. D. thesis (University of Illinois, 1978) (unpublished).

[25]Scotchcast 8 epoxy, 3M Company, Saint Paul, Minn. 55101.

[26]General Radio 1615A capacitance bridge and 1311A audio oscillator along with a Princeton Applied Research 5204 dual phase lock-in synchronous detector. The internal oscillator of the lock-in was used to trigger the audio oscillator.

[27]Lake Shore Cryotronics, Inc., 4949 Freeway Drive East, Columbus, Ohio 43229.

[28]A. C. Anderson, R. E. Peterson, and J. E. Robichaux, Rev. Sci. Instrum. 41, 528 (1970).

[29]R. J. Soulen, J. F. Schooley, and G. A. Evans, Rev. Sci. Instrum. 44, 1537 (1973).

[30]J. F. Schooley, J. Phys. (Paris) 39, C6-1169 (1978).

[31]J. C. Wang, J. B. Bates, and T. Kaneda, Bull. Am. Phys. Soc. 23, 241 (1978).

[32]J. Jackle, Z. Phys. 257, 212 (1972).

[33]A. S. Barker, J. A. Ditzenberger, and J. P. Remeika, Phys. Rev. B 14, 386 (1976).

[34]D. B. McWhan, S. M. Shapiro, J. P. Remeika, and G. Shirane, J. Phys. C 8, L487 (1975); C. H. Hao and L. L. Chase, Bull. Am. Phys. Soc. 23, 242 (1978).

[35]To explain the thermal-conductivity data above 5 K requires two assumptions beyond the tunneling-states model: that high-frequency phonons transport heat only weakly, and that phonon-phonon scattering dominates the high-temperature thermal conductivity of K β-alumina. See Refs. 16 and 24.

[36]R. J. Grant, I. M. Hodge, M. D. Ingram, and A. R. West, Nature 266, 42 (1977), and references cited.

[37]U. Strom, P. C. Taylor, S. G. Bishop, T. L. Reinecke, and K. L. Ngai, Phys. Rev. B 13, 3329 (1976).

[38]M. S. Whittingham and R. A. Huggins, J. Chem. Phys. 54, 414 (1971); J. Electrochem. Soc. 118, 1 (1971).